Simulation of radiation transfer and coherent backscattering in nematic liquid crystals

E. V. Aksenova,* D. I. Kokorin,† and V. P. Romanov‡

Saint Petersburg State University, Department of Physics, Ul'yanovskaya, 1, Petrodvoretz, Saint Petersburg, 198504, Russia

(Received 4 December 2013; published 15 May 2014)

We consider the multiple scattering of light by fluctuations of the director in a nematic liquid crystal. Using methods of numerical simulation the peak of the coherent backscattering and the coefficients of anisotropic diffusion are calculated. The calculations were carried out without simplifying assumptions on the properties of the liquid crystal. The process of multiple scattering was simulated as a random walk of photons in the medium. We investigated in detail the transition to the diffusion regime. The dependence of the diffusion coefficients on the applied magnetic field and the wavelength of light were studied. The results of simulation showed a nonmonotonic dependence of the diffusion coefficients on the external magnetic field. For calculation of the peak of the coherent backscattering we used the semianalytical approach as long as in nematic liquid crystals this peak is extremely narrow. The parameters of the backscattering peak and of diffusion coefficients which were found in numerical simulations were compared with the experimental data and the results of analytical calculation.

DOI: 10.1103/PhysRevE.89.052506 PACS number(s): 42.70.Df, 78.20.Bh, 42.25.Bs, 42.25.Fx

I. INTRODUCTION

The study of multiple scattering of light in liquid crystals has attracted considerable attention for many years [1–10]. Nematic liquid crystals (NLCs) have been studied most thoroughly. Physical properties of these systems are well known, and as a rule their elastic and optical parameters are measured with high accuracy. From the point of view of multiple scattering liquid crystals are the unique objects. In these systems the multiple scattering occurs on the thermal fluctuations of the orientation. The amplitude and correlation properties of these fluctuations are studied in detail both experimentally and theoretically. NLCs differ from suspensions where the scattering takes place on the separate particles and from heterogeneous solid dielectrics where the scattering occurs on the structural inhomogeneities.

The difficulty of studying multiple scattering in NLCs is due to the large optical anisotropy and the complex structure of the phase function of the single scattering on the fluctuations of the director.

The most interesting and well-investigated effects of multiple scattering in NLCs are the coherent backscattering and the diffusion of light.

An effective description of the radiative transfer in a strongly inhomogeneous media provides the method of the diffusion approximation. This approach was comprehensively studied in a number of papers [11–18]. The speed of photon diffusion and diffusion coefficients are obtained in experiments on the passage of the short pulses through the medium [19]. In isotropic systems the diffusion coefficient is determined by the relation $D = vl_{tr}/3$, where v is the velocity of light in the inhomogeneous medium and l_{tr} is the transport length. In absorbing media the ratio $D = v/[3(\mu_s' + \mu_a)]$ is used for the diffusion coefficient D where μ_s' and μ_a are the coefficients of scattering and absorption. The correctness of this expression was discussed in a series of papers [20–22].

Considerable interest has been attracted to the study of the diffusion of photons in NLCs. This problem has been discussed in Refs. [1–6,8,9,13,23]. For calculation of the diffusion coefficients two approaches were proposed. One approach was based on the exact analogy between the wave problem and the electron-impurity problem, for which the exact solution for the diffusion constant is expressed by means of the Kubo-Greenwood formula [3–5,24]. Another approach was based on the approximate solution of the Bethe-Salpeter integral equation [1,2]. The components of the diffusion tensor were measured by the pulse method in Refs. [25,26] and by the deformation of the light beam passing through the sample in Ref. [1].

The effect of coherent backscattering was thoroughly studied theoretically and experimentally for different systems [27–29], including liquid crystals [2,3,8,9,30]. Calculation of the backscattering peak is reduced to the summation of ladder and cyclic diagrams. This problem is solved exactly for a system of pointlike scatterers [13] while for the scatterers of finite size or fluctuations with finite correlations length it is necessary to introduce approximations. The accuracy of these approximations is not always possible to control due to the complexity of the problem being considered.

On the other hand there exist numerical simulation methods [1,4,5,8,31] that allow one to overcome many difficulties occurring in the analytical approach. Due to the extreme complexity of the problem both analytical and numerical methods were performed using some simplifying assumptions. Despite these simplifications, the authors showed the tensor nature of the diffusion coefficient and obtained the narrow peak of coherent backscattering with an elliptical shape in cross section. However, with the emergence of the experimental data on the investigation of the diffusion of light and of the coherent backscattering the question arises whether the results of the theory, numerical simulation, and experiment are consistent with each other. The most natural solution of this problem seems the numerical simulation of multiple scattering of light in NLCs without any simplifying assumptions. In the process of numerical simulations we will take into account the scattering up to very high orders. Therefore the calculation results allow us to establish reliably the values of diffusion

*aksev@mail.ru
†dmitry@kokorin.org
‡vpromanov@mail.ru

coefficients and to describe in detail the shape of the coherent backscattering peak. The aim of our study was to solve this problem and to compare with the results of analytical and numerical calculations and with the experiment.

The paper is organized as follows. The second part describes the method of numerical simulation. The third part contains description of the transition to the diffusion approximation and discusses the dependence of the diffusion tensor on the system parameters. The fourth part contains the results of numerical simulation of coherent backscattering. The conclusion contains the analysis of the obtained results. The basic equations describing the fluctuations in a NLC, its optical properties, and single light scattering are presented in the Appendix.

II. SIMULATION OF SCATTERING IN ANISOTROPIC MEDIUM

We have simulated the multiple scattering by the Monte Carlo method. In our study of the photon diffusion we assumed that the entire space is occupied by NLCs oriented by the magnetic field. In this case such an approach is justified since the tensor diffusion (A13) is a macroscopic quantity and it is independent of the size of the sample. When studying the coherent backscattering it was considered that an NLC fills a half space.

The standard simulation procedure of the multiple scattering is as follows. Between scatterings the photon propagates along a straight line. The length passed by a photon between successive scatterings is generated randomly so that the average distance between successive scatterings coincides with the mean free path of a photon $l_{(j)} = \tau_{(j)}^{-1}(\mathbf{k}^{(i)})$. Choice of the direction for the photon propagation after scattering is also a random quantity and depends on the single-scattering phase function.

In our problem this procedure is much more complicated. As long as the medium is uniaxial there exist two types of waves, i.e., ordinary and extraordinary in the scattering process. The value of the wave vector of extraordinary wave depends on the angle between the direction of the wave propagation and that of the vector director. The phase function of the single scattering of this wave depends on the angle between the direction of the optical axis and the wave vectors of the incident and of the scattered waves. Finally, the mean free path of a photon $l_{(j)}$ determined by the extinction depends on the type of the wave and the direction of its propagation. The angular dependence of the extinction coefficient in Eq. (A11) determines both the LC optical anisotropy and the modules of orientation elasticity. This dependence does not disappear even if we neglect the difference between the Frank modules [5,31]. Figure 1 shows the angular dependence of extinction for different ratios between the Frank modules and the same optical anisotropy.

According to our model prior to each act of scattering a photon is in one of two "channels" of scattering, i.e., it has one of two polarizations, (o) or (e). If prior to scattering a photon had (e) polarization it can be scattered into one of two channels, (o) or (e). At the start of simulations we calculate the probability of $(e) \to (e)$ scattering. This probability $w(\theta_i)$ is determined as a ratio of the scattering intensity in the extraordinary wave and the total scattering intensity:

$$w(\theta_i) = \frac{\int I_{(e)}^{(e)}\, d\mathbf{\Omega}_\mathbf{q}}{\int \left(I_{(e)}^{(e)} + I_{(e)}^{(o)}\right) d\mathbf{\Omega}_\mathbf{q}}, \tag{2.1}$$

where θ_i is the angle between $\mathbf{k}^{(i)}$ and $\mathbf{n}_0$.

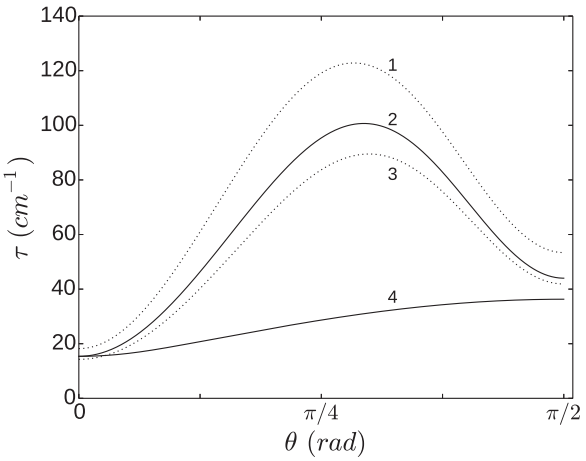

FIG. 1. Angular dependence of extinction of the ordinary (curve 4) and extraordinary (curves 1–3) rays. Calculations are carried out by Eq. (A11) for the following values of the parameters $\varepsilon_\perp = 2.2$, $\varepsilon_a = 0.8$, $\lambda = 4.88 \times 10^{-5}$ cm, $T = 301$ K, $H = 5000$ Oe, $\chi_a = 1.38 \times 10^{-7}$. The Frank moduli are as follows: $K_{11} = 0.79\, K_{33}$, $K_{22} = 0.43\, K_{33}$, $K_{33} = 6.1 \times 10^{-7}$ dyn for curves 2 and 4; $K_{11} = 2.6 \times 10^{-7}$ dyn, $K_{22} = 1.4 \times 10^{-7}$ dyn for curve 1; and $K_{11} = K_{22} = K_{33} = 4.5 \times 10^{-7}$ dyn for curve 3 (one constant approximation). In all three cases, the sum of the Frank moduli is the same.

Between successive scatterings the photons move in a medium with permittivity $\varepsilon(\mathbf{k})$. At each scattering event it is necessary determined randomly the direction of the photon propagation, the type of the wave into which it is supposed to scatter, and the distance of its free path.

The probability density of the scattering per unit solid angle is given by the phase function of the single scattering. As far as the investigated system is anisotropic this probability depends on the angle θ_i between the wave vector $\mathbf{k}^{(i)}$ prior to the scattering and the vector director $\mathbf{n}$.

Usually the generation of a random variable with a given probability density is performed using the inverse function method [32]. Typically in this approach a model phase function (for example, the Henyey-Greenstein phase function) is used [33–35]. In our case expression for the phase function (A5) is much more complicated. Therefore generation of random directions in each scattering event leads to a cumbersome procedure including the conversion of special functions such as elliptic integrals. For this reason this approach seems to be hopeless for numerical simulation.

In the general case in order to describe the single scattering it is necessary to define four parameters: two angles determining the direction of the vector $\mathbf{k}^{(i)}$ and the two angles determining the vector $\mathbf{k}^{(s)}$. As far as our system is optically uniaxial there is a symmetry consisting in that the simultaneous rotation vectors $\mathbf{k}^{(i)}$ and $\mathbf{k}^{(s)}$ around the director $\mathbf{n}$ do not change the scattering probability for $\mathbf{k}^{(i)}$ to $\mathbf{k}^{(s)}$. This allows us to reduce the number of parameters from four to three. As one

of the parameters we choose the angle θ_i. For a given vector $\mathbf{k}^{(i)}$ we introduce a local Cartesian coordinate system with unit vectors

$$\mathbf{v}_3 = \frac{\mathbf{k}^{(i)}}{k^{(i)}}, \quad \mathbf{v}_1 = \mathbf{v}_3 \times \mathbf{n}, \quad \mathbf{v}_2 = \mathbf{v}_3 \times \mathbf{v}_1. \tag{2.2}$$

Within this coordinate system the corresponding spherical coordinate system is introduced. The angles θ and ϕ of this coordinate frame will be used for description of the scattering direction. Thus in order to generate a random direction of the photon after the scattering it is necessary for a given angle θ_i to randomly get the angles θ and ϕ defining the direction of $\mathbf{k}^{(s)}$. For the angle ϕ it is sufficient to consider the interval $[0,\pi]$ since expression (A5) has a mirror symmetry relative to the point $\phi = \pi$.

Owing to the complexity of the expression (A5) we have built an approximation of the phase function. For this purpose we took into account that it smoothly depends on the angle θ_i. In order to interpolate the phase function (A5) we create initially a discrete set of angles $\{\tilde{\theta}_1,\tilde{\theta}_2,\ldots\tilde{\theta}_M\}$ for the angle θ_i, such that within the intervals $\tilde{\theta}_j \leqslant \theta_i \leqslant \tilde{\theta}_{j+1}$ the phase function changes by less than 1%. For each angle $\tilde{\theta}_j$ in this set we divide the solid angle of scattering $\theta \in [0,\pi]$, $\phi \in [0,\pi]$ into rectangular cells s^j:

$$s^j : \theta \in \left[\theta_l^j,\theta_r^j\right), \quad \phi \in \left[\phi_l^j,\phi_r^j\right), \tag{2.3}$$

where the indices l and r refer to the left and the right edges of the rectangle. The sizes of the rectangles are chosen so that the bilinear interpolation of the phase function $I^j(\theta,\phi)$ constructed from the values calculated at the vertices of the cell described the phase function with the required accuracy. The division was carried out adaptively so that a narrow peak of the phase function had a sufficiently large number of cells because photons are scattered primarily in this direction. The construction of interpolation was performed separately for each type of scattering.

In our simulations the accuracy of the interpolation was about 1%. This precision was achieved for the number of cells $3 \times 10^3 - 3 \times 10^4$.

In simulating each act of a single scattering for the angle θ_i we select the closest element of the set $\{\tilde{\theta}_1,\tilde{\theta}_1,\ldots,\tilde{\theta}_M\}$ and this way we get the corresponding interpolation of $I^j(\theta,\phi|\theta_i)$.

The probability that the direction of scattering enters the cell s^j is equal to

$$p_j = \frac{\int_{\phi,\theta\in s^j} I^j(\theta,\phi|\theta_i)\,d\Omega}{\sum_t \int_{\phi,\theta\in s^t} I^t(\theta,\phi|\theta_i)\,d\Omega}. \tag{2.4}$$

With the aid of the uniform random number generator in the interval $[0,1]$ we select the cell with the number t of the array such that

$$\sum_{j=1,j<t} p_j < r, \qquad \sum_{j=1,j\leqslant t} p_j \geqslant r, \tag{2.5}$$

where r is a random number. After selection of the cell it is necessary to choose random angles θ and ϕ inside the cell. This can be done by using a two-dimensional analog of the inverse function method [32] using the corresponding bilinear interpolation of the cell I^t as the probability density. Thus the obtained angles θ and ϕ belonging to this cell will determine the direction of the photon propagation after the last scattering.

On having determined the wave vector of the scattered photon $\mathbf{k}^{(s)}$ it is necessary to get the distance that the photon passes before the next scattering event. The probability density distribution of the mean free path between two successive scattering events s has the form [32]

$$f(s) = \frac{1}{l}\exp(-s/l), \tag{2.6}$$

where l is the mean free path. Then the probability that the mean free path of a photon exceeds s is

$$\xi = \int_s^\infty f(s')\,ds', \tag{2.7}$$

where ξ is a random number uniformly distributed within the range $(0,1]$. So explicit expression for s is obtained from Eqs. (2.6) and (2.7):

$$s = -l\ln\xi. \tag{2.8}$$

The expression (2.8) allows us to receive the lengths of the free path of photons with the given probability density (2.6).

So in our simulation we first choose the scattering channel, then the direction of scattering, and finally the distance that the photon would run before the next scattering.

For simulations of the multiple scattering by fluctuations of the director in an NLC we calculated phase function without any simplifying assumptions. In contrast to Ref. [5] our approach allows us to perform the calculations for arbitrary values of the Frank moduli and to take into account the dependence on the azimuthal angle in the $(e) \to (e)$ scattering.

To control the accuracy in the phase function we performed more fine crushing of the polar and azimuthal angles. The crushing process was stopped when the results of calculations ceased to change.

III. RADIATIVE TRANSFER IN THE DIFFUSION APPROXIMATION

In the studying of the photon diffusion the purpose of simulation is to investigate the statistical features of radiation transfer in an anisotropic medium. For this purpose we run randomly a separate photon and determine its trajectory by the method described in the previous section. The procedure is repeated many times in order to get a set of trajectories. With the help of this set we calculate the mean square displacement of photons along and across to the director, $\langle r_\parallel^2\rangle$ and $\langle \mathbf{r}_\perp^2\rangle$. It is known that starting from a certain moment of time the scattered radiation can be described within the framework of the diffusion approximation. It means that the mean square displacement of photons starts to depend linearly on time. In this case the following relations are valid:

$$\langle x^2\rangle = \langle r_\parallel^2\rangle = 2D_\parallel t, \tag{3.1}$$

$$\langle y^2\rangle + \langle z^2\rangle = \langle \mathbf{r}_\perp^2\rangle = 4D_\perp t. \tag{3.2}$$

Here the direction of the x axis is chosen along the director. The performed calculation allows us to study the transition to the diffusion regime with increasing the scattering order. Also we investigate the dependence of the diffusion coefficients on the external field and on the wavelength of light [36].

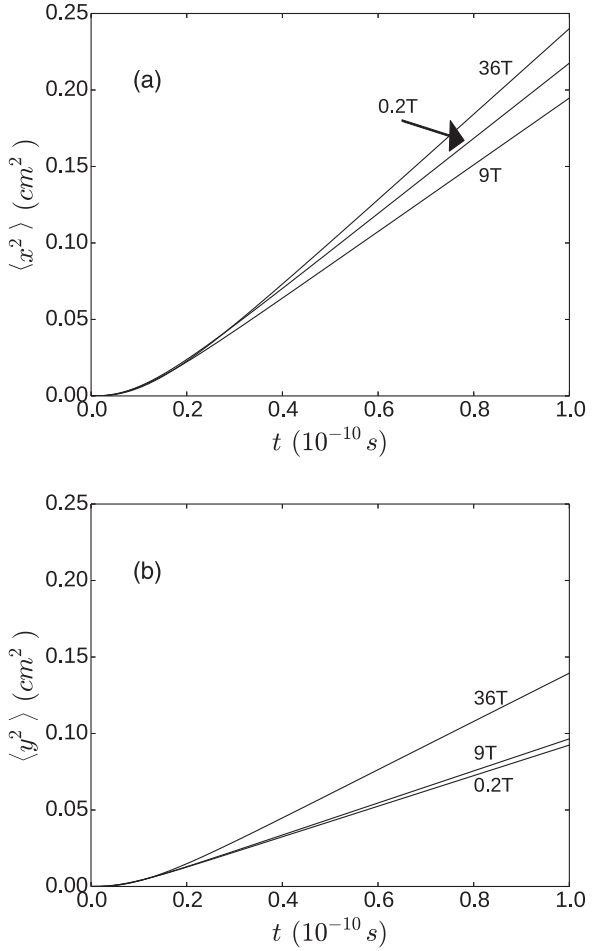

FIG. 2. Plots of the mean square displacement of the photons (a) along and (b) across the director vs time for three values of the external magnetic field.

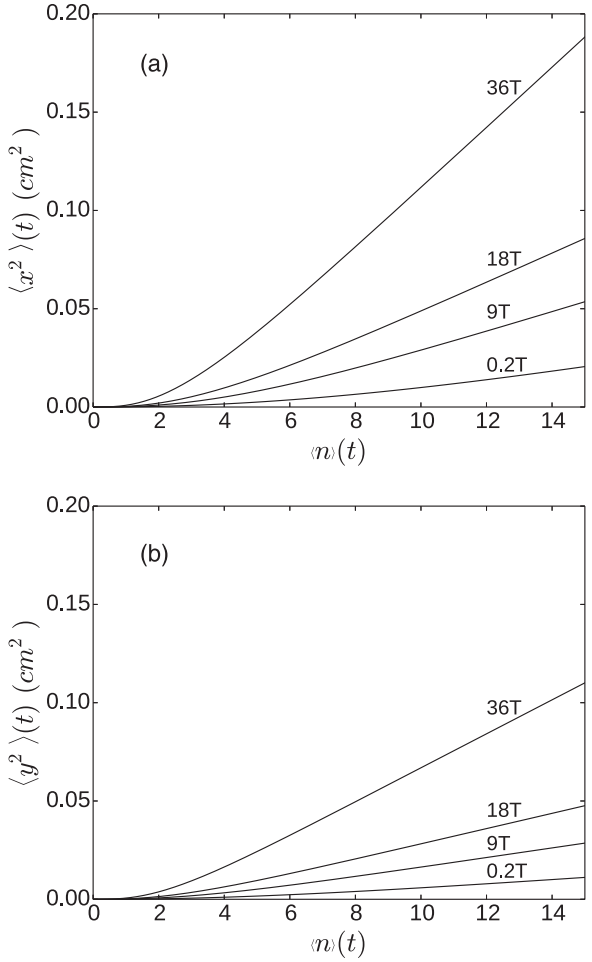

FIG. 3. Plots of the mean square displacement of the photons (a) along and (b) across the director vs the mean number of scattering events for three values of external magnetic fields. The plots were obtained in the following way. The number of scatterings, n, and the square of photon coordinates, x^2 and y^2, were calculated for each trajectory and for each moment of time. These values were averaged over the trajectories, and $\langle n \rangle(t)$, $\langle x^2 \rangle(t)$, $\langle y^2 \rangle(t)$ were obtained for each t.

Figure 2 shows the time dependence of the mean squared displacement of the photon along (a), and across (b), the director for three values of external magnetic field. In Fig. 3 the same value as a function of the average scattering orders is presented. The calculations are performed for the liquid crystal 5CB with the following parameters: $K_{33} = 7.5 \times 10^{-7}$ dyn, $K_{11} = 0.79K_{33}$, $K_{22} = 0.43K_{33}$, $\chi_a = 1.1 \times 10^{-7}$, $\varepsilon_\parallel = 3.0$, $\varepsilon_\perp = 2.2$, $\lambda = 514.5$ nm, and $T = 301$ K. The interval of linear dependence in both figures correspond to areas where the diffusion approximation is valid. In the simulation process all photons are emitted in the same direction, which is taken for the z axis.

It is seen that the initial part of the square displacement of photons does not linearly depends on time. It means that in this interval the diffusion regime has not yet established. Note that the forms of the curves in Figs. 2 and 3 do not coincide. The reason is that the transition from the time scale to the scale of scattering orders is rather complicated. The reason is that the passage time between successive scatterings of photons depends on the direction of propagation. For the extraordinary beam it is due to dependence of the refractive index and the extinction coefficient on the angle between the wave vector and the director. For an ordinary beam it is caused by the angular dependence of the extinction coefficient only.

It is seen that the number of scattering orders which are required for transition to the diffusion regime decreases with increasing of magnetic field. This result is natural since with increasing the magnetic field the phase function of the single scattering approaches to circular one, and consequently the randomization of the photon propagation directions occurs for a smaller number of scatterings.

We also studied the dependence of the transition rate to the diffusion regime on the direction of photon emission from the source. It was found that the time of transition to a diffusive regime is smaller if the photon is emitted by the small angle with respect to the vector director. We present functions $\langle x^2 \rangle(t)$ for the four directions of emission of photons in Fig. 4. The calculations are performed for the same parameters as in Fig. 2 and $H = 0.2$ T.

The diffusion coefficients were found from the array of data corresponding to the diffusive regime by the method of the maximum likelihood using the explicit form of the Green

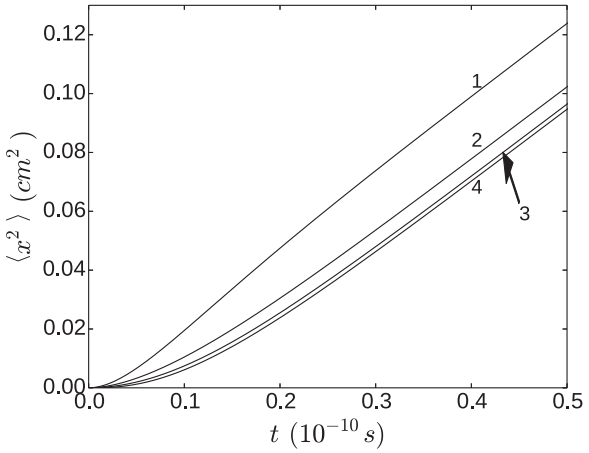

FIG. 4. Dependence of the mean square displacement of the photon, $\langle x^2 \rangle$, on angle θ between the incident beam and the director: (1) $-\theta = \pi/12$, (2) $-\theta = \pi/4$, (3) $-\theta = \pi/3$, and (4) $-\theta = \pi/2$.

function (A14) of the diffusion equation. They were found from the relations

$$D_\perp = \frac{1}{4MN}\sum_{j=1}^{M}\frac{1}{t_j}\sum_{l=1}^{N} r_{\perp l}^2(t_j) = \frac{1}{4M}\sum_{j=1}^{M}\frac{1}{t_j}\langle r_\perp^2(t_j)\rangle, \quad (3.3)$$

$$D_\parallel = \frac{1}{2MN}\sum_{j=1}^{M}\frac{1}{t_j}\sum_{l=1}^{N} r_{\parallel l}^2(t_j) = \frac{1}{2M}\sum_{j=1}^{M}\frac{1}{t_j}\langle r_\parallel^2(t_j)\rangle, \quad (3.4)$$

where N is the number of radiated photons, M is the number of time steps, the index l is the number of photons, and the index j is the time step. In our calculation the discrete time points t_j are introduced starting from $t = t_0$ with a constant step Δt. Here time $t = t_0$ belongs to the region of the diffusion regime. In general we can choose a rather arbitrary set of values of t_j as long as for such separate trajectories it is not difficult to determine the position of the photon at each moment.

All calculations for the diffusion coefficients are performed for the same parameters as in Fig. 2. Figure 5 shows the

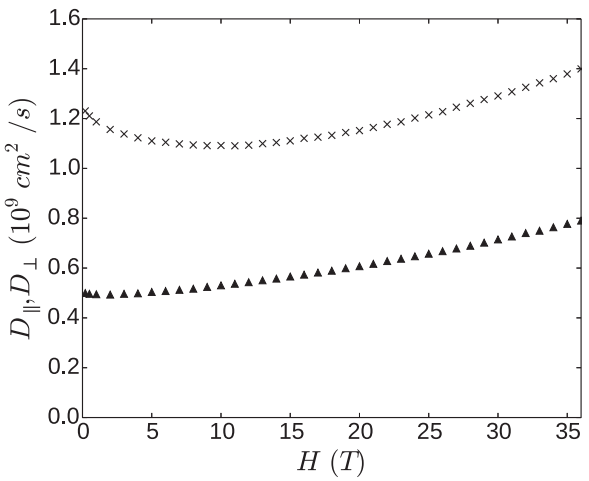

FIG. 5. Dependence of the diffusion coefficients of photons $D_\parallel$ ($\times$) and $D_\perp$ (▲) on the magnetic field.

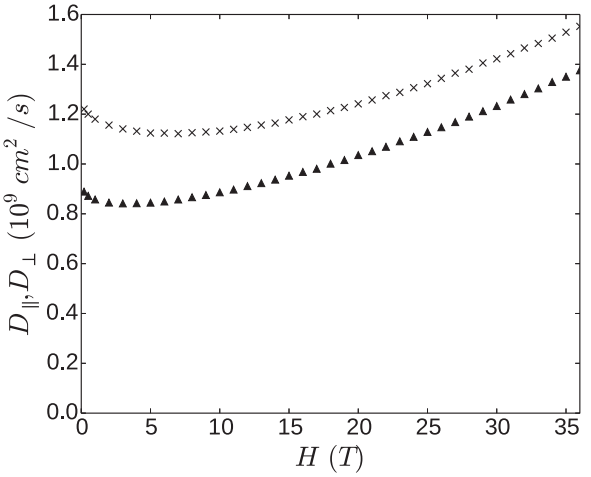

FIG. 6. Dependence of the diffusion coefficients of photons $D_\parallel$ ($\times$) and $D_\perp$ (▲) on the magnetic field calculated with regard to the (e) rays only.

dependence of the diffusion coefficients on the magnetic field. The figure shows that the diffusion coefficients vary nonmonotonically with increase of the field. One can see that nonmonotonic behavior disappears for the strong fields. The reason is that in this case the phase function of the single scattering becomes close to the circular one and the director fluctuations are suppressed by the external field. In order to determine the cause of the nonmonotonic behavior we have tried to simplify the system which was used in the simulation. Figure 6 shows the results of the calculation when only $(e) \rightarrow (e)$ scattering is taken into account. The results when in addition one-constant approximation is used are shown in Fig. 7. It is seen that the nonmonotonic dependence of the light diffusion coefficients on the magnetic field holds. The observed nonmonotonic behavior of the diffusion coefficient does not agree with the results of calculation in Refs. [1,2], where smooth growth of $D_\parallel$ and $D_\perp$ with increasing of the field

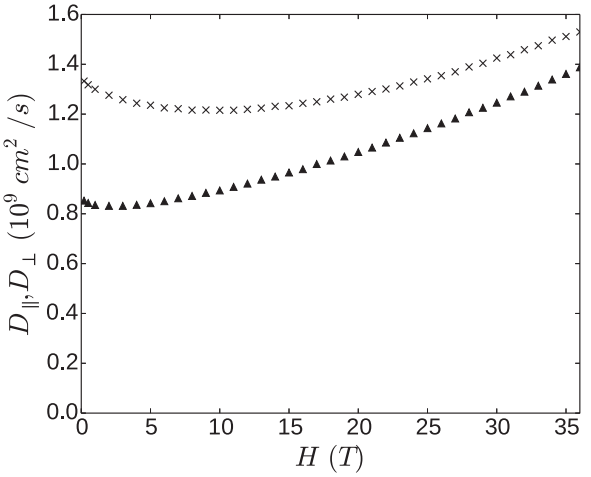

FIG. 7. Dependence of the diffusion coefficients of photons $D_\parallel$ ($\times$) and $D_\perp$ (▲) on the magnetic field calculated with regard to the (e) rays only. Simulations are performed for one constant approximation ($K_{11} = K_{22} = K_{33} = 5.55 \times 10^{-7}$ dyn).

is predicted. Perhaps such a discrepancy is due to the fact that in Refs. [1,2] only the minimal eigenvalue of the integral operator of the Bethe-Salpeter equation was taken into account.

At first glance, a significant nonmonotonic behavior of the diffusion coefficients $D_\parallel$ and $D_\perp$ in the region of relatively small fields is not consistent with the results of analytical calculations of the diffusion tensor (see Ref. [2], Fig. 7). In this paper the Bethe-Salpeter integral equation was solved taking into account the lowest eigenvalue. This solution presents the series of the spherical harmonics. When calculating the diffusion coefficients, the contributions of the first two nonzero harmonics were taken into account. It was shown that the dependence of the second harmonic on the field has a rather complicated nonmonotonic character (see Ref. [2], Fig. 5). However, the contribution of this harmonic was too small to significantly affect the field dependence of the diffusion coefficients. Numerical simulation actually corresponds to an iterative solution of the Bethe-Salpeter equation in the ladder approximation. Formally, this solution contains the contributions of all spherical harmonics. Probably for this reason we obtained a significant nonmonotonic dependence of the diffusion coefficients on the field.

We also investigated the dependence of the diffusion coefficients on the wavelength of light. The results of the calculations are shown in Fig. 8. It is seen that within the visible light spectrum the diffusion coefficients vary almost twice. This means that in quantitative calculations this effect can be essential.

In order to illustrate the reliability of the obtained results we calculated the diffusion coefficient using the designed program for a simple model.

We will consider a scalar isotropic model for which the diffusion coefficient has the form

$$D = \frac{v}{3}\frac{1}{\mu_s'} = \frac{v}{3}\frac{l_{\text{ext}}}{1-\langle\cos\theta\rangle}, \tag{3.5}$$

where l_{ext} is the extinction length, and $\langle\cos\theta\rangle$ is the average cosine of the scattering angle. Instead of a correlation function of the permittivity fluctuations (A8) we accept the scalar

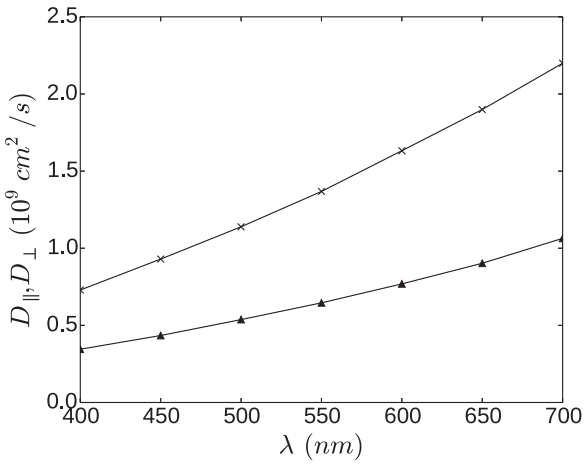

FIG. 8. Dependence of the diffusion coefficients of photons $D_\parallel$ (×) and $D_\perp$ (▲) on the radiation wavelength for $H = 0.2$ T.

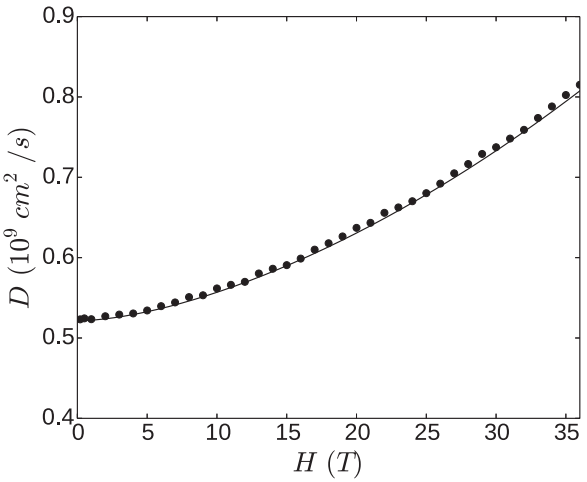

FIG. 9. Dependence of the diffusion coefficient on the external magnetic field for the scalar model (3.6). Solid line is the result of calculations by Eq. (3.7).

expression

$$B = \frac{k_0^4\varepsilon_a^2 k_B T}{Kq^2 + \chi_a H^2}, \tag{3.6}$$

where $q = 2k_0\sqrt{\varepsilon_\perp}\sin(\theta/2)$, θ is the scattering angle. For this model, the diffusion coefficient has the form

$$D = \frac{16\pi c K\sqrt{\varepsilon_\perp}}{3k_0^2\varepsilon_a^2 k_B T}\frac{1}{2-h^2\ln(1+2/h^2)}, \tag{3.7}$$

where $h^2 = \chi_a H^2/(2\varepsilon_\perp k_0^2 K)$.

For this model we calculate the dependence of the diffusion coefficient on the field using Eq. (3.7) and using the program that was created earlier for simulation of the multiple scattering of light in NLCs. For calculations we used the following parameters: $K = 5.55\times10^{-7}$ dyn, $\varepsilon_\perp = 2.2$, $k_0 = 2\pi/\lambda$, $\lambda = 514.5$ nm, $\chi_a = 1.1\times10^{-7}$, $T = 301$ K. The results presented in Fig. 9 coincide within fractions of a percent.

Comparisons were performed for three liquid crystals: 5CB, PAA, and MBBA. Table I shows the parameters of these liquid crystals, the external conditions, and the obtained results. The dashes mean that in the cited papers the corresponding data are not presented. In the right part of the table the data are arranged in pairs. In the upper row of each pair the results of numerical simulations are shown, and in the lower row the known theoretical or experimental data are presented. The sole exception is line 4 where the simulation results are compared with two types of experiments. In the first experiment the diffusion coefficients and their ratio were measured by the passage of a light pulse through the NLC. In the second experiment only the ratio of the diffusion coefficients was obtained by investigating the distribution of the light transmitted through the liquid crystal layer. The experiment of the same type was completed in Ref. [1] (line 3 of the table). Note that the simulation results are in reasonable agreement with the theory for the coefficient $D_\perp$ (lines 1, 5, and 6 of the table). For the coefficient $D_\parallel$ the results of simulation are noticeably larger than predicted by theoretical calculations. Furthermore simulation results differ markedly

TABLE I. Comparison of the calculated and measured diffusion coefficients of photons. The Frank modules K_{jj} are measured in 10^{-7} dyn. The diffusion coefficients are measured in 10^9 cm^2/s.

No.	NLC	$\varepsilon_\parallel$	$\varepsilon_\perp$	K_{11}	K_{22}	K_{33}	H,T	ξ,μm	λ,nm	T,K	Results of	$D_\parallel$	$D_\perp$	$D_\parallel/D_\perp$
1				4.187	2.279						Simulation	1.93	0.87	2.28
		2.923	2.381			5.3	0.5	4.72	546.4	300	Theory [1,6]	1.43	0.98	1.45
2				2.3							Simulation	1.70	0.75	2.21
											Theory [6]	–	–	1.51
3	5CB	2.923	2.381	4.187	2.279	5.3		11.8			Simulation	1.75	0.78	2.26
		–	–	–	–	–	0.2	–	514.5	303.15	Experiments [1]	0.7 ± 0.1	0.5 ± 0.1	1.6 ± 0.25
4		2.923	2.381	5.93	3.23	7.5		5.22			Simulation	1.54	0.68	2.26
		–	–	–	–	–	0.5	–	405	300	Experiments [25,26]	0.456 ± 0.019	0.362 ± 0.015	1.26
											Experiments [25]	–	–	1.44 ± 0.06
5	PAA	3.35	2.47	3.0		9.51	–	2.2	500	400	Simulation	0.67	0.28	2.43
											Theory [4]	0.502	0.287	1.75
6	MBBA	4.7	5.4	3.7		7.45	–	1.5	500	300	Simulation	1.54	0.88	1.77
											Theory [4]	1.146	0.872	1.31

from the experimental data (lines 3 and 4 of the table). The possible reason is that some parameters of the NLC used in the experiments were not indicated and the simulation was performed with the data taken from Ref. [37].

IV. THE FORMATION OF THE COHERENT BACKSCATTERING PEAK

The main feature of calculating the coherent backscattering peak in NLCs is that noticeable interest in scattering of photons emitted from the medium presents the scattering extremely close to the normal, i.e., at angles $\sim 10^{-4}$–10^{-6} rad. After multiple scattering the probability of photon emission in such a narrow range of angles is very small. Therefore the direct numerical procedure based on a simple counting of photons in this range of angles is extremely inefficient, and in order to solve this problem a semianalytical Monte Carlo [38] method is used [39]. The idea of this method is as follows. We take into account the contribution $\delta_n(\mathbf{k}_F^{(s)})$ of each photon into intensity at each scattering event in the direction $\mathbf{k}_F^{(s)}$ in the range of angles $\theta_s < 10^{-4}$ rad that we are interested in

$$\delta_n\left(\mathbf{k}_F^{(s)}\right) = W_n\, p_{is}\left(\mathbf{k}^{(i)},\mathbf{k}_F^{(s)}\right) \exp\left[-\frac{1}{l_s\left(\mathbf{k}_F^{(s)}\right)}\frac{z_n}{\cos\theta_s}\right], \qquad (4.1)$$

where n is the scattering order, W_n is the weight of a photon, p_{is} is the normalized single scattering phase function, $\mathbf{k}_F^{(s)}$ is the wave vector of scattering directed to the receiver at an angle θ_s, and z_n is the distance between the current position of the photon and the boundary. The angle θ_s is measured strictly from the backscattering direction $0 \leqslant \theta_s \leqslant \pi/2$. Equation (4.1) has a simple physical meaning. The contribution of the photon $\delta_n(\mathbf{k}_F^{(s)})$ is the product of three factors: the probability of a photon W_n to suffer n scatterings without abandoning the medium; the probability p_{is} to have the direction of the scattering $\mathbf{k}_F^{(s)}$; and the exponential factor meaning the probability to reach the boundary without experiencing collisions. It should also be taken into account that a photon contributes to a (o) or (e) scattering canal.

Calculations have shown that in our system the photons are emitted from the medium mainly after a small number of scatterings, $n \sim 10^2$. On the other hand a significant contribution to the coherent backscattering yields the photons that have experienced a very large number of scatterings $n \sim 10^4$–10^5. For better accounting for these photons we used a modified procedure of simulation in which the photons do not abandon the medium [38]. In this condition we take into account the weakening of the intensity caused by the weight W_n. The condition of keeping the photons in the medium is reached in the following way. If the current scattering is directed to the boundary, $k_z^{(s)} < 0$, then the length of the free path is generated between 0 and the distance from the current starting point and the boundary.

For the photon located at a distance z from the boundary and having a wave vector $\mathbf{k}^{(i)}$ before the scattering the probability to leave the medium at each scattering event is expressed as

$$\mathrm{esc}\left(\mathbf{k}^{(i)},z\right) = \sum_{s=o,e}\int_0^{\pi/2}\sin\theta_s\, d\theta_s \int_0^{2\pi} d\phi_s\, p_{is}\left(\mathbf{k}^{(i)},\mathbf{k}^{(s)}\right) \times \exp\left[-\frac{1}{l_s(\mathbf{k}^{(s)})}\frac{z}{\cos\theta_s}\right], \qquad (4.2)$$

where ϕ_s is the azimuthal angle measured from the axis x. It is convenient to calculate the function $\mathrm{esc}(\mathbf{k}^{(i)},z)$ preliminarily in the form of an interpolation table. This function provides determination of the decrease in weight for the photon after each next step of scattering

$$W_{n+1} = W_n\left[1 - \mathrm{esc}(\mathbf{k}^{(i)},z)\right], \quad W_1 = 1. \qquad (4.3)$$

The expression (4.3) takes into account the loss of intensity due to emission of photons from the medium.

We assume that the detector that collects the radiation is infinite and occupies the whole plane XY. We are interested in the distribution of the photons emitted from the medium over angles θ_s and ϕ_s. For each emitted photon we collect the emission angles θ_s, ϕ_s, and vector $\mathbf{R}_s^{(n)}$ which indicate the place of the photon emission from the medium. Vector $\mathbf{R}_s^{(n)}$ lies on the surface of the medium, $R_{s,z}^{(n)} = 0$. Summation of the contributions of photons $\delta_n(\mathbf{k}_F^{(s)})$ (4.1) in the direction θ_s, ϕ_s yields the angular distribution of the intensity in the ladder approximation. The corresponding contribution of the cyclic

diagrams is assumed to be obtained by multiplying $\delta_n(\mathbf{k}_F^{(s)})$ by the phase factor $\cos[\mathbf{q}\cdot(\mathbf{R}_s^{(n)}-\mathbf{R}_i)]$ [40,41], where vector $\mathbf{R}_i$ indicates the place of the photons' incidence, its coordinates are taken as $\mathbf{R}_i=(0,0,0)$, $\mathbf{q}$ is the scattering vector $\mathbf{q}=\mathbf{k}_F^{(s)}-\mathbf{k}_0^{(i)}$, and $\mathbf{R}_i$. Summing over all the photons for each pair of angles θ_s and ϕ_s we get the angular dependence of the relative intensity of the scattered radiation [12,13]

$$J(\theta_s,\phi_s)=\frac{J_C+J_L}{J_L}, \tag{4.4}$$

where J_L and J_C are the contributions of the ladder and cyclic diagrams

$$J_L=\sum_{a=1}^{A}\sum_{j=1}^{n}\delta_j\left(\mathbf{k}_F^{(s)}\right), \tag{4.5}$$

$$J_C=\sum_{a=1}^{A}\sum_{j=2}^{n}\delta_j\left(\mathbf{k}_F^{(s)}\right)\cos\left[\mathbf{q}\cdot\mathbf{R}_s^{(j)}\right]. \tag{4.6}$$

It should be recalled that the cyclic diagrams are formed starting from the double scattering. Here the summation over $a=1,2,\ldots,A$ means the sum over all photons participating in the simulation. The summation over j is performed over the orders of scattering. In the simulation we restrict ourselves by $n=10^5$ scattering orders. In addition if the contribution to the scattering of the order δ_j becomes very small, $\sim 10^{-8}$, then the higher orders for this photons are not taken into account.

The angular dependence of the scattered radiation intensity was obtained from Eq. (4.4). Figure 10 shows the dependence of the intensity on the angle θ_s for two cross sections of the peak at $\phi_s=\pi/2$ and $\phi_s=0$, curves 3 and 4. It is seen that there is a noticeable anisotropy of scattering. The calculations were performed for the liquid crystal 5CB studied in Refs. [8,9]. Parameters of this liquid crystal are $K_{11}=0.79K_{33}$, $K_{22}=0.43K_{33}$, $K_{33}=6.1\times10^{-7}$ dyn, $H=0.5$ T, $\chi_a=1.38\times10^{-7}$, $\varepsilon_a=0.8$, $\varepsilon_\perp=2.2$, $\lambda=488$ nm, $T=301$ K. The experimental sample was a cylinder of 8 cm diameter and 4 cm height. The extinction for such a liquid crystal is shown in Fig. 1, curve 2 for the extraordinary beam and curve 4 for the ordinary beam. The figure shows that the mean free path of a photon is of order $l\sim2\times10^{-2}$ cm, and it is significantly less than the sample size. Therefore in the simulation of the experiment the approximation of the semi-infinite medium is quite justified. Figure 10 also shows the results of analytical calculations, curves 1 and 2 [30], and experimental data [8,9], curves 5 and 6. In the selected geometry the contribution of the single scattering (e)→(e) in the strictly backward direction is absent. In analytical calculations the (e)→(e) was only taken into account. The contributions of the ladder and the cyclic diagrams in this case are equal, and the relative peak height should be equal to 2. In Refs. [8,9] this height was about 1.6. Probably this could be caused by the finite width of the instrumental function of the device. From Fig. 10 one can see that the results of the analytical calculations, lines 1 and 2, predict a peak width which differs from the numerical calculations. Probably the cause is that in the summation of the diagram series a number of assumptions have been made. Among them are the diffusion approximation [2] and a simplified model for the pair correlation function.

The calculated anisotropy of the backscattering peak is shown in Fig. 11. The cross sections of the peak are shown at different heights: 1.7, 1.6, 1.5, and 1.4. The calculated anisotropy of the peak is 1.46; in the experiment the anisotropy was 1.17 ± 0.04.

Performed numerical simulations allow us to retrieve the details of the process which are practically impossible to obtain both experimentally and theoretically. In particular Fig. 12 shows the forming of the coherent backscattering peak when we take into account a different number of scattering orders. All curves are normalized to the intensity determined by summing of the ladder diagrams of all scattering orders, i.e., $n=10^5$. We see the noticeable contribution made to the lower orders of scattering. These contributions are not described

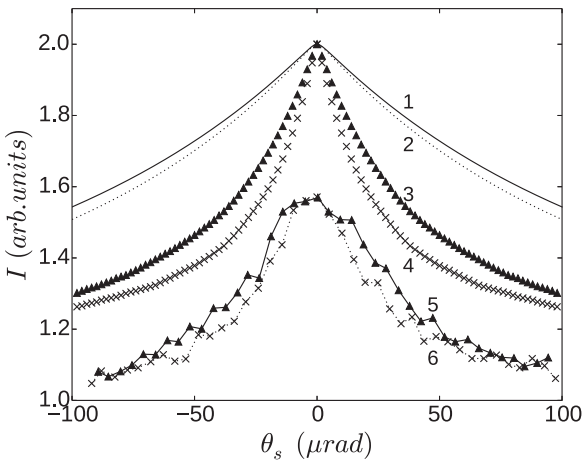

FIG. 10. Cross sections of the coherent backscattering peaks. Here curves (1) and (2) were obtained analytically [30], curves (3) and (4) are the results of simulations, and curves (5) and (6) are the experimental data [8,9]. The curves (1), (3), and (5) refer to the angle $\phi_s=0$, and the curves (2), (4), and (6) refer to the angle $\phi_s=\pi/2$.

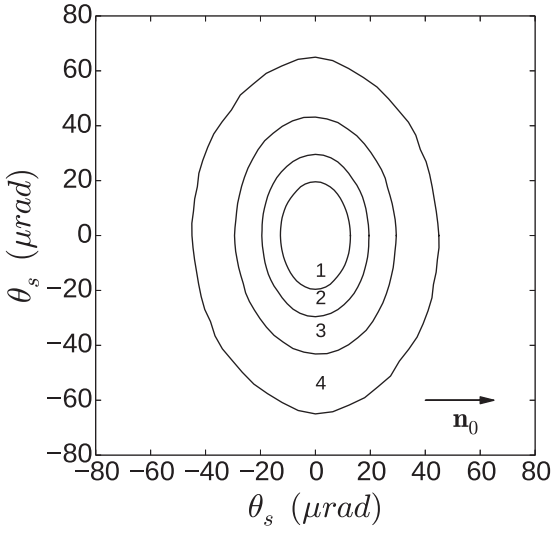

FIG. 11. Cross sections of a coherent backscattering peak obtained by numerical simulation in polar coordinates (θ_s,ϕ_s). Cross sections by planes perpendicular to the z axis are calculated at heights of $J=1.7$ (1), 1.6 (2), 1.5 (3), and 1.4 (4).

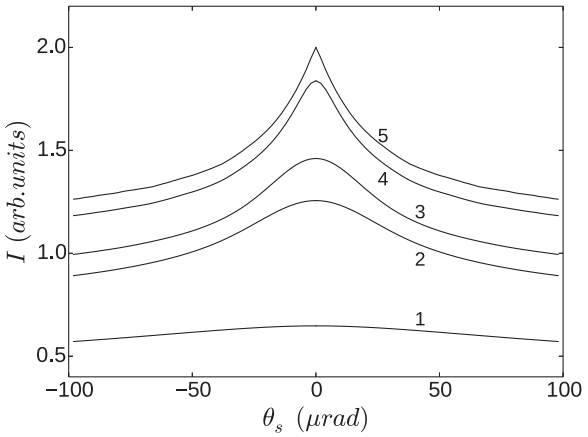

FIG. 12. The contribution of the first n scattering orders to the formation of the backscattering peak: (1) $n = 10$, (2) $n = 50$, (3) $n = 10^2$, (4) $n = 10^3$, and (5) $n = 10^5$. All the curves are normalized by the sum of ladder diagrams that take into account $n = 10^5$ scatterings.

in the framework of the diffusion approximation as it was shown in the previous section. It means that the analytical calculations performed in the diffusion approximation cannot fit the experimental curves with considerable accuracy.

V. CONCLUSION

We have investigated the multiple scattering of light in NLCs with the aid of a computer simulation method. Calculating the multiple scattering of photons we take into account the very high scattering orders (up to 10^5).

The transition from radiative transfer in the form of contributions of separate scattering orders to the photon diffusion in the inhomogeneous media has been studied in detail.

We make a simulation based on actual parameters of the liquid crystal without introduction of any simplifying assumptions. The phase function was taken into account with a high accuracy. Considerable attention was paid to study the dependence of the diffusion tensor on the external magnetic field. The simulation results show that the field dependence becomes nonmonotonic in weak fields. This nonmonotonic behavior remains when we introduce the simplifying assumptions such as the one-constant approximation and the scattering of the extraordinary beams only.

In Ref. [2] it was shown that the contributions of the spherical harmonics of higher orders to the diffusion coefficients are nonmonotonically dependent on the field. However, the contribution of the third spherical harmonic only is of the order of 1%. In numerical simulations we actually take into account the spherical harmonics of all orders. Probably therefore in our calculations the nonmonotonic behavior of the diffusion coefficients occurs in the weak fields.

For the reliability control we performed the calculations for a simple scalar model. For this model it is known the analytical expression for the diffusion coefficient. The diffusion coefficients obtained using our program and calculated analytically coincide with high accuracy.

It was found that the diffusion coefficients vary significantly with the wavelength within the region of the visible light.

In the analysis of the diffusion tensor dependence on the magnetic field calculations were carried out up to the fields when the values of the orientational and of the field contributions to the energy are comparable. It corresponds to an anomalously high value of the field. The reason is that all estimates refer to the diamagnetic liquid crystals, which have very low anisotropy of magnetic susceptibility. At present paramagnetic liquid crystals based on rare-earth elements are synthesized in which the anisotropy of magnetic susceptibility has much greater values. For these liquid crystals even a strong field region is quite available for experimental research.

We also carried out a comparison of the diffusion coefficients obtained by numerical simulation with those that were obtained for the liquid crystals in the theoretical calculations in the works and in a real experiment.

Besides the light diffusion we study the coherent backscattering in NLC by numerical simulation. Simulation allowed us to analyze the contributions of different orders of scattering in the formation of the backscattering peak. The semianalytical approach allowed us to take into account the contributions of very high scattering orders (up to 10^5). These contributions are important in the formation of the backscattering peak.

ACKNOWLEDGMENTS

The authors acknowledge Saint Petersburg State University for Research Grant No. 11.37.145.2014 and the Russian Foundation for Basic Research for Grant No. 12-02-01016-a. We thank Prof. P. N. Vorontsov-Velyaminov for useful remarks.

APPENDIX: DIRECTOR FLUCTUATIONS AND SINGLE LIGHT SCATTERING IN NEMATIC LIQUID CRYSTALS

The orientation of the liquid crystal is determined by the unit vector director $\mathbf{n}(\mathbf{r})$. The free energy of distortion in an external magnetic field has the form [42]

$$F = \frac{1}{2}\int d\mathbf{r}\{K_{11}(\operatorname{div}\mathbf{n})^2 + K_{22}(\mathbf{n}\cdot\operatorname{rot}\mathbf{n})^2 + K_{33}(\mathbf{n}\times\operatorname{rot}\mathbf{n})^2 - \chi_a(\mathbf{n}\cdot\mathbf{H})^2\}. \quad \text{(A1)}$$

Here $K_{ll}, l = 1,2,3$ are Frank modules, $\chi_a = \chi_\parallel - \chi_\perp$, $\chi_\parallel, \chi_\perp$ are the magnetic susceptibilities along and normal to $\mathbf{H}$, and $\mathbf{H}$ is the constant external magnetic field. It is assumed that the sample is large enough so that we can ignore the interaction energy with the anchoring surface. We consider that $\chi_a > 0$. In equilibrium the vector director $\mathbf{n} = \mathbf{n}^0$ is constant, and for $\chi_a > 0$ it is directed along the magnetic field, $\mathbf{n}^0 \parallel \mathbf{H}$.

As an optical system the nematic liquid crystal is uniaxial with a permittivity tensor

$$\varepsilon_{\alpha\beta}(\mathbf{r}) = \varepsilon_\perp\delta_{\alpha\beta} + \varepsilon_a n_\alpha(\mathbf{r})n_\beta(\mathbf{r}), \quad \text{(A2)}$$

where $\varepsilon_a = \varepsilon_\parallel - \varepsilon_\perp$, $\varepsilon_\parallel, \varepsilon_\perp$ are permittivities along and across the director $\mathbf{n}^0$.

Eigenwaves $\mathbf{E}^0(\mathbf{r})$ in a uniaxial media are two plane waves, i.e., ordinary, (o), and extraordinary, (e), with wave vectors

$\mathbf{k}^{(o)}$ and $\mathbf{k}^{(e)}$:

$$\mathbf{E}^0_{(j)} = E^0_{(j)}\mathbf{e}^{(j)}e^{i\mathbf{k}^{(j)}\cdot\mathbf{r}}, \quad j = o,e.$$

Here $E^0_{(j)}$ is the amplitude of the field, $\mathbf{e}^{(j)}$ is the unit polarization vector, $k^{(j)} = k_0 n^{(j)}$,

$$n^{(o)} = \sqrt{\varepsilon_\perp}, \quad n^{(e)} = \sqrt{\frac{\varepsilon_\parallel\varepsilon_\perp}{\varepsilon_\perp + \varepsilon_a\cos^2\theta_e}} \tag{A3}$$

are refractive indices of the ordinary and the extraordinary waves, and θ_j is the angle between the vectors $\mathbf{n}^0$ and $\mathbf{k}^{(j)}$.

The fluctuations of the permittivity tensor are mainly caused by the fluctuations of the director and have the form

$$\delta\varepsilon_{\alpha\beta}(\mathbf{r}) = \varepsilon_{\alpha\beta}(\mathbf{r}) - \varepsilon^0_{\alpha\beta} = \varepsilon_a\left[n^0_\alpha\delta n_\beta(\mathbf{r}) + n^0_\beta\delta n_\alpha(\mathbf{r})\right], \tag{A4}$$

where $\varepsilon^0_{\alpha\beta} = \varepsilon_\perp\delta_{\alpha\beta} + \varepsilon_a n^0_\alpha n^0_\beta$.

The intensity of the single scattering by fluctuations of the permittivity $\delta\hat{\varepsilon}(\mathbf{r})$ is equal to

$$I^{(s)}_{(i)} = I^0_{(i)}\frac{V_{sc}}{(4\pi)^2R^2}\frac{1}{n^{(i)}\cos\delta^{(i)}} \times \sum_{j=o,e}\frac{n^{(j)}}{\cos^3\delta^{(j)}}f^2_{(j)}e^{(s)}_\alpha e^{(s)}_\beta B_{\alpha\beta\mu\nu}(\mathbf{q})e^{(i)}_\mu e^{(i)}_\nu, \tag{A5}$$

$$\mathbf{e}^{(o)} = \frac{\mathbf{n}\times\mathbf{s}^{(o)}}{\sin\theta_o}, \qquad \mathbf{e}^{(e)} = \frac{\mathbf{s}^{(e)}\varepsilon_\parallel\cos\theta_e - \mathbf{n}(\varepsilon_\parallel\cos^2\theta_e + \varepsilon_\perp\sin^2\theta_e)}{\sin\theta_e(\varepsilon^2_\parallel\cos^2\theta_e + \varepsilon^2_\perp\sin^2\theta_e)^{1/2}}, \tag{A6}$$

where indices $i,s = (o,e)$ show the type of the incident and the scattered waves, V_{sc} is the scattering volume, R is the distance between the scattering volume and the point of observation,

$$\cos\delta^{(o)} = 1, \quad \cos\delta^{(e)} = \frac{\left(\mathbf{e}^{(e)}\hat{\varepsilon}^0\mathbf{e}^{(e)}\right)^{1/2}}{n^{(e)}}, \tag{A7}$$

$\mathbf{q} = \mathbf{k}^{(s)} - \mathbf{k}^{(i)}$, $\mathbf{k}^{(s)}$ and $\mathbf{k}^{(i)}$ are the wave vectors of the scattered and the incident wave, $I^0_{(i)}$ is the intensity of the incident light, and $B_{\alpha\beta\mu\nu}(\mathbf{q}) = k_0^4\langle\delta\varepsilon_{\alpha\mu}\delta\varepsilon^*_{\nu\beta}\rangle(\mathbf{q})$ is the correlation function of the permittivity fluctuations. It is determined by the fluctuations of the director according to the expression

$$B_{\alpha\gamma\beta\delta}(\mathbf{q}) = k_0^4\varepsilon_a^2\sum_{l=1}^{2}\langle|\delta n_l(\mathbf{q})|^2\rangle\left(a_{l\alpha}a_{l\gamma}n^0_\beta n^0_\delta + a_{l\alpha}a_{l\delta}n^0_\beta n^0_\gamma + a_{l\beta}a_{l\delta}n^0_\alpha n^0_\gamma + a_{l\beta}a_{l\gamma}n^0_\alpha n^0_\delta\right). \tag{A8}$$

Here

$$\langle|\delta n_l(\mathbf{q})|^2\rangle = \frac{k_BT}{K_{ll}q^2_\perp + K_{33}q^2_\parallel + \chi_aH^2}, \quad l = 1,2, \tag{A9}$$

$$\mathbf{a}_1(\mathbf{q}) = \frac{\mathbf{q}}{q}, \quad \mathbf{a}_2(\mathbf{q}) = \mathbf{n}^0\times\mathbf{a}_1(\mathbf{q}), \qquad f_{(o)} = 1, \quad f^2_{(e)} = \frac{\left(\mathbf{s}^{(e)}\hat{\varepsilon}^0\mathbf{s}^{(e)}\right)\left(\mathbf{s}^{(e)}\hat{\varepsilon}^{02}\mathbf{s}^{(e)}\right)}{\varepsilon_\parallel\varepsilon_\perp}, \tag{A10}$$

where the unit vector $\mathbf{s}^{(j)} = \mathbf{k}^{(j)}/k^{(j)}$ is directed along the wave vector.

If we substitute the explicit expression for the correlation function in the formula for intensity of the single light scattering (A5), it is easy to see that there is no scattering of the ordinary ray into the ordinary one, (o)→(o), since the vector director $\mathbf{n}^0$ and the polarization vector of the ordinary ray are orthogonal. Note that the scattering (o)→(e) and (e)→(o) occur for the vector $\mathbf{q}$ with the length $q \sim k_0|n^{(o)} - n^{(e)}|$. It means that the scattering vector at all angles remains finite. At the same time the intensity of scattering (e)→(e) for small angles has a sharp peak. The height of this peak increases with decreasing of the field, $H \to 0$. In this case the scattering of the extraordinary ray into an extraordinary one is mainly forward.

If we ignore the intrinsic absorption, the extinction coefficient is determined by the loss of light due to scattering and it has the form [2]

$$\tau_{(j)}(\mathbf{k}^{(j)}) = \frac{1}{(4\pi)^2}\frac{e^{(j)}_\alpha e^{(j)}_\beta}{n^{(j)}\cos^2\delta^{(j)}} \times \sum_{l=o,e}\int d\Omega^{(l)}_{\mathbf{q}}\frac{n^{(l)}e^{(l)}_\nu e^{(l)}_\mu}{\cos^2\delta^{(l)}}B_{\alpha\beta\nu\mu}\left(\mathbf{k}^{(l)} - \mathbf{q}\right), \tag{A11}$$

where $\int d\Omega^{(l)}_{\mathbf{q}}$ denotes the integration over the surface $q = k^{(l)}(\mathbf{q})$.

When light propagates in rather thick samples of NLCs the multiple scattering regime is formed as far as the director fluctuations are not small. In order to describe the intensity of the multiple scattering it is convenient to use the Bethe-Salpeter equation. In the weak scattering approximation the Bethe-Salpeter equation can be solved by iteration. The solution has the form of an infinite series. The terms of this series correspond to the contributions of different scattering orders. In the diffusion approximation the probability density $P = P(\mathbf{r},t)$ of the arrival for a photon at point $\mathbf{r}$ at time t is described by the diffusion equation

$$\frac{\partial P}{\partial t} = D_\parallel\nabla^2_\parallel P + D_\perp\nabla^2_\perp P, \tag{A12}$$

where $\hat{D}$ is the tensor diffusion coefficient of light, which for NLC has the form

$$\hat{D} = D_\perp\hat{I} + (D_\parallel - D_\perp)\mathbf{n}^0\otimes\mathbf{n}^0, \tag{A13}$$

where $D_\parallel$ and $D_\perp$ are the diffusion coefficients along and across $\mathbf{n}^0$. In the case of a point source in an infinite medium the solution of this equation is

$$P(\mathbf{r},t) = \frac{1}{8(\pi t)^{3/2}D_\perp D_\parallel^{1/2}}\exp\left[-\frac{1}{4t}\left(\frac{r^2_\parallel}{D_\parallel} + \frac{r^2_\perp}{D_\perp}\right)\right], \tag{A14}$$

where $r_\parallel$ and $\mathbf{r}_\perp$ are the directions along and across the director.

The solution of the Bethe-Salpeter equation in the diffusion approximation allows us to describe multiple scattering of light in all directions except a narrow vicinity of the backscattering. In this area the effect of the coherent backscattering becomes significant. This effect means that the fields scattered by the same inhomogeneities in reverse order are coherent with fields scattered in the direct order. This leads to additional contribution to the scattering and the emerging of a narrow peak in the backscattering region.

[1] H. Stark, M. H. Kao, K. A. Jester, T. C. Lubensky, and A. G. Yodh, J. Opt. Soc. Am. A **14**, 156 (1997).
[2] H. Stark and T. C. Lubensky, Phys. Rev. E **55**, 514 (1997).
[3] B. A. van Tiggelen, R. Maynard, and A. Heiderich, Phys. Rev. Lett. **77**, 639 (1996).
[4] B. A. van Tiggelen, A. Heiderich, and R. Maynard, Mol. Cryst. Liq. Cryst. **293**, 205 (1997).
[5] A. Heiderich, R. Maynard, and B. A. van Tiggelen, J. Phys. II (France), **7**, 765 (1997).
[6] B. van Tiggelen and H. Stark, Rev. Mod. Phys. **72**, 1017 (2000).
[7] L. V. Kuz'min, V. P. Romanov, and L. A. Zubkov, Phys. Rev. E **54**, 6798 (1996).
[8] R. Sapienza, D. S. Wiersma, and D. Delande, Mol. Cryst. Liq. Cryst. **429**, 193 (2005).
[9] R. Sapienza, S. Mujumdar, C. Cheung, A. G. Yodh, and D. Wiersma, Phys. Rev. Lett. **92**, 033903 (2004).
[10] B. A. van Tiggelen and S. E. Skipetrov (eds.), *Wave Scattering in Complex Media: From Theory to Applications*, NATO Science Series II, Mathematics, Physics and Chemistry (Kluwer Academic Publishers, Dordrecht, 2003).
[11] M. J. Stephen, Phys. Rev. Lett. **56**, 1809 (1986).
[12] M. J. Stephen and G. Cwilich, Phys. Rev. B **34**, 7564 (1986).
[13] F. C. MacKintosh and S. John, Phys. Rev. B **37**, 1884 (1988).
[14] K. Furutsu, Phys. Rev. A **39**, 1386 (1989).
[15] K. M. Yoo, Feng Liu, and R. R. Alfano, Phys. Rev. Lett. **64**, 2647 (1990).
[16] Z. Q. Zhang, I. P. Jones, H. P. Schriemer, J. H. Page, D. A. Weitz, and P. Sheng, Phys. Rev. E **60**, 4843 (1999).
[17] X. Zhang and Z. Q. Zhang, Phys. Rev. E **66**, 016612 (2002).
[18] S. Gerritsen and G. E. W. Bauer, Phys. Rev. E **73**, 016618 (2006).
[19] A. Z. Genack and J. M. Drake, Europhys. Lett. **11**, 331 (1990).
[20] T. Durduran, A. G. Yodh, B. Chance, and D. A. Boas, J. Opt. Soc. Am. A **14**, 3358 (1997).
[21] D. J. Durian, Opt. Lett. **23**, 1502 (1998).
[22] R. Aronson and N. Corngold, J. Opt. Soc. Am. A **16**, 1066 (1999).
[23] A. Mertelj and M. Copic, Phys. Rev. E **75**, 011705 (2007).
[24] G. D. Mahan, *Many Particle Physics* (Plenum, New York, 1981), Section 7.1.C.
[25] D. S. Wiersma, A. Muzzi, M. Colocci, and R. Righini, Phys. Rev. Lett. **83**, 4321 (1999).
[26] D. S. Wiersma, A. Muzzi, M. Colocci, and R. Righini, Phys. Rev. E **62**, 6681 (2000).
[27] M. P. Van Albada and A. Lagendijk, Phys. Rev. Lett. **55**, 2692 (1985).
[28] P. E. Wolf and G. Maret, Phys. Rev. Lett. **55**, 2696 (1985).
[29] V. L. Kuz'min and V. P. Romanov, Phys. Usp. **39**, 231 (1996).
[30] E. V. Aksenova, V. L. Kuz'min, and V. P. Romanov, JETP **108**, 516 (2009).
[31] V. L. Kuz'min and A. Yu. Val'kov, Opt. Spectr. **111**, 465 (2011).
[32] J. E. Gentle, *Random Number Generation and Monte Carlo Methods* (Springer, New York, 2003).
[33] A. Ishimaru, *Wave Propagation in Random Media* (Academic, New York, 1978).
[34] S. E. Skipetrov and S. S. Chesnokov, Quantum Electron. **28**, 733 (1998).
[35] I. V. Meglinski, V. L. Kuzmin, D. Y. Churmakov, and D. A. Greenhalgh, Proc. R. Soc. A **461**, 43 (2005).
[36] For numerical simulation of photon diffusion the program https://github.com/DmitryKokorin/diffmc/ has been developed.
[37] M. J. Bradshaw, E. P. Raynes, J. D. Bunning, and T. E. Faber, J. Physique **46**, 1513 (1985).
[38] E. Tinet, S. Avrillier, and J. M. Tualle, J. Opt. Soc. Am. A **13**, 1903 (1996).
[39] For numerical simulation of coherent backscattering the program https://github.com/DmitryKokorin/scatmc2/ has been developed.
[40] G. Maret and P. E. Wolf, Zs. Phys. B **65**, 409 (1987).
[41] D. J. Pine, D. A. Weitz, J. X. Zhu, and E. J. Herbolzheimer, Physique **51**, 2101 (1990).
[42] P. G. de Gennes and J. Prost, *The Physics of Liquid Crystals* (Clarendon Press, Oxford, 1993).